X-Ray Imaging and Spectroscopy Mission

Collaborators: Audard, Marc; Eckert, Dominique; Ferrigno, Carlo; Paltani, Stéphane

How to cite

Collab. X-Ray Imaging and Spectroscopy Mission. In: Publications of the Astronomical Society of Japan, 2025, p. psaf023. doi: 10.1093/pasj/psaf023

This publication URL: https://archive-ouverte.unige.ch/unige:185646
Publication DOI: 10.1093/pasj/psaf023

Publications of the Astronomical Society of Japan, 2025, **00**(0), 1–9
https://doi.org/10.1093/pasj/psaf023
Advance access publication date: 2025 April 11

X-Ray Imaging and Spectroscopy Mission

Makoto Tashiro,[1,2,*] Richard Kelley,[3] Shin Watanabe,[1] Hironori Maejima,[1] Lillian Reichenthal,[3] Kenichi Toda,[1] Leslie Hartz,[3] Andrea Santovincenzo,[4] Kyoko Matsushita,[5] Hiroya Yamaguchi,[1] Robert Petre,[3] Brian Williams,[3] Matteo Guainazzi,[4] Elisa Costantini,[6] Yoh Takei,[1] Yoshitaka Ishisaki,[7] Ryuichi Fujimoto,[1] Joy Henegar-Leon,[3] Gary Sneiderman,[3] Hiroshi Tomida,[1] Koji Mori,[8] Hiroshi Nakajima,[9] Yukikatsu Terada,[1,2] Matthew Holland,[3] Michael Loewenstein,[2,10] Eric Miller,[11] Makoto Sawada,[12] Timothy Kallman,[3] Jelle Kaastra,[6,13] Chris Done,[14] Teruaki Enoto,[15] Aya Bamba,[16] Lia Corrales,[17] Yoshihiro Ueda,[15] Erin Kara,[11] Irina Zhuravleva,[18] Yutaka Fujita,[7] Yoshitaka Arai,[1] Marc Audard,[19] Hisamitsu Awaki,[20] Ralf Ballhausen,[2,10] Chris Baluta,[3] Nobutaka Bando,[1] Ehud Behar,[21] Thomas Bialas,[3] Rozenn Boissay-Malaquin,[3] Laura Brenneman,[22] Gregory V. Brown,[23] Meng Chiao,[3] Renata Cumbee,[3,22] Cor de Vries,[4] Jan-Willem den Herder,[6] María Díaz Trigo,[24] Michael DiPirro,[3] Tadayasu Dotani,[1] Jacobo Ebrero Carrero,[4] Ken Ebisawa,[1] Megan Eckart,[23] Dominique Eckert,[19] Satoshi Eguchi,[25] Yuichiro Ezoe,[7] Carlo Ferrigno,[19] Adam Foster,[22] Yasushi Fukazawa,[26] Kotaro Fukushima,[1] Akihiro Furuzawa,[27] Luigi Gallo,[28] Javier Garcia Martinez,[3] Nathalie Gorter,[6] Martin Grim,[6] Liyi Gu,[6] Kouichi Hagino,[16] Kenji Hamaguchi,[3,10] Isamu Hatsukade,[8] Katsuhiro Hayashi,[1] Takayuki Hayashi,[3,10] Natalie Hell,[23] Edmund Hodges-Kluck,[3,10] Takafumi Horiuchi,[1] Ann Hornschemeier,[3] Akio Hoshino,[1] Yuto Ichinohe,[29] Chisato Ikuta,[1] Ryo Iizuka,[1] Daiki Ishi,[1] Manabu Ishida,[1] Naoki Ishihama,[1] Kumi Ishikawa,[7] Kosei Ishimura,[30] Tess Jaffe,[3] Satoru Katsuda,[2] Yoshiaki Kanemaru,[1] Steven Kenyon,[3] Caroline Kilbourne,[3] Mark Kimball,[3] Shunji Kitamoto,[12] Shogo Kobayashi,[3] Takayoshi Kohmura,[31] Aya Kubota,[32] Maurice Leutenegger,[3] Yoshitomo Maeda,[1] Maxim Markevitch,[3] Hironori Matsumoto,[33] Keiichi Matsuzaki,[1] Dan McCammon,[34] Brian McLaughlin,[3] Brian McNamara,[35] Francois Mernier,[36] Joseph Miko,[3] Jon Miller,[17] Kenji Minesugi,[1] Shinji Mitani,[1] Ikuyuki Mitsuishi,[37] Misaki Mizumoto,[38] Tsunefumi Mizuno,[39] Koji Mukai,[3] Hiroshi Murakami,[40] Richard Mushotzky,[10] Kazuhiro Nakazawa,[37] Chikara Natsukari,[1] Jan-Uwe Ness,[41] Kenichiro Nigo,[42] Mari Nishiyama,[1] Kumiko Nobukawa,[43] Masayoshi Nobukawa,[44] Hirofumi Noda,[45] Hirokazu Odaka,[33] Mina Ogawa,[1] Shoji Ogawa,[1] Anna Ogorzalek,[3,10] Takashi Okajima,[3] Atsushi Okamoto,[42] Naomi Ota,[46] Masanobu Ozaki,[1] Stephane Paltani,[19] Paul Plucinsky,[22] F. Scott Porter,[3] Katja Pottschmidt,[3,10] Jose Antonio Quero,[4] Takahiro Sasaki,[1] Kosuke Sato,[2,47] Rie Sato,[1] Toshiki Sato,[48] Yoichi Sato,[42] Hiromi Seta,[7] Maki Shida,[1] Megumi Shidatsu,[20] Shuhei Shigeto,[1] Russel Shipman,[6] Keisuke Shinozaki,[43] Peter Shirron,[3] Aurora Simionescu,[6] Randall Smith,[22] Yang Soong,[3] Hiromasa Suzuki,[1] Andrew Szymkowiak,[49] Hiromitsu Takahashi,[26] Mai Takeo,[50] Toru Tamagawa,[29] Keisuke Tamura,[3,51] Takaaki Tanaka,[52] Atsushi Tanimoto,[53] Yuichi Terashima,[20] Yohko Tsuboi,[54] Masahiro Tsujimoto,[1] Hiroshi Tsunemi,[33] Takeshi Tsuru,[15] Hiroyuki Uchida,[15] Nagomi Uchida,[1] Yuusuke Uchida,[5] Hideki Uchiyama,[55] Shinichiro Uno,[56] Jacco Vink,[57] Michael Witthoeft,[3] Rob Wolfs,[6] Satoshi Yamada,[29] Shinya Yamada,[12] Kazutaka Yamaoka,[37] Noriko Yamasaki,[1] Makoto Yamauchi,[8] Shigeo Yamauchi,[46] Keiichi Yanagase,[42] Tahir Yaqoob,[3,51] Susumu Yasuda,[42] Tomokage Yoneyama,[54] Tessei Yoshida,[1] and Miohoko Yukita[3]

Received: 2025 February 1; **Accepted:** 2025 March 14

[1]Institute of Space and Astronautical Science (ISAS), Japan Aerospace Exploration Agency (JAXA), 3-1-1 Yoshinodai, Chuo-ku, Sagamihara, Kanagawa 252-5210, Japan
[2]Department of Physics, Saitama University, 255 Shimo-Okubo, Sakura, Saitama, Saitama 338-8570, Japan
[3]NASA/Goddard Space Flight Center, MD 20771, USA
[4]European Space Agency (ESA), European Space Research and Technology Centre (ESTEC), 2200 AG Noordwijk, The Netherlands
[5]Department of Physics, Tokyo University of Science, 1-3 Kagurazaka, Shinjuku-ku, Tokyo 162-8601, Japan
[6]SRON Netherlands Institute for Space Research, Niels Bohrweg 4, 2333 CA Leiden, The Netherlands
[7]Department of Physics, Tokyo Metropolitan University, 1-1 Minami-Osawa, Hachioji-shi, Tokyo 192-0397, Japan
[8]Faculty of Engineering, University of Miyazaki, 1-1 Gakuen-kibanadai-nishi, Miyazaki, Miyazaki 889-2192, Japan
[9]College of Science and Engineering, Kanto Gakuin University, 1-50-1 Mutsuura-higashi, Kanazawa-ku, Yokohama, Kanagawa 236-8501, Japan
[10]Department of Astronomy, University of Maryland, 4296 Stadium Dr., College Park, MD 20742, USA
[11]Kavli Institute for Astrophysics and Space Research, Massachusetts Institute of Technology, 70 Vassar St, Cambridge, MA 02139, USA
[12]Department of Physics, Rikkyo University, 3-34-1 Nishi Ikebukuro, Toshima-ku, Tokyo 171-8501, Japan
[13]Leiden Observatory, University of Leiden, PO Box 9513, NL-2300 RA Leiden, The Netherlands
[14]Department of Physics, Durham University, Durham DH1 3LE, UK
[15]Department of Physics, Kyoto University, Kitashirakawa Oiwakecho, Sakyo-ku, Kyoto, Kyoto 606-8502, Japan
[16]Department of Physics, The University of Tokyo, 7-3-1 Hongo, Bunkyo-ku, Tokyo 113-0033, Japan
[17]Department of Astronomy, University of Michigan, 323 West Hall, 1085 S University Ave, Ann Arbor, MI 48109, USA
[18]Department of Astronomy and Astrophysics, University of Chicago, 5640 S Ellis Ave, Chicago, IL 60637, USA
[19]Department of Astronomy, University of Geneva, Chemin Pegasi, 51, Versoix CH-1290, Switzerland
[20]Department of Physics, Ehime University, 2-5 Bunkyo-cho, Matsuyama, Ehime 790-8577, Japan
[21]Department of Physics, Technion, Technion City, Haifa 3200003, Israel
[22]Harvard-Smithsonian Center for Astrophysics, 60 Garden Street, Cambridge, MA 02138, USA
[23]Lawrence Livermore National Laboratory, 7000 East Ave, Livermore, CA 94550, USA
[24]ESO, Karl-Schwarzschild-Strasse 2, 85748 Garching bei München, Germany
[25]Department of Economics, Kumamoto Gakuen University, 2-5-1 Oe, Chuo-ku, Kumamoto, Kumamoto 862-8680, Japan
[26]Department of Physics, Hiroshima University, 1-3-1 Kagamiyama, Higashi-Hiroshima, Hiroshima 739-8526, Japan
[27]Department of Physics, Fujita Health University, 1-98 Dengakugakubo, Kutsukake-cho, Toyoake, Aichi 470-1192, Japan
[28]Department of Astronomy and Physics, Saint Mary's University, 923 Robie St Halifax, Nova Scotia B3H 3C3, Canada
[29]RIKEN Nishina Center, 2-1 Hirosawa, Wako, Saitama 351-0198, Japan
[30]Faculty of Science and Engineering, Waseda University, 3-4-1 Okubo, Shinjuku-ku, Tokyo 169-8555, Japan
[31]Department of Physics, Tokyo University of Science, 2641 Yamazaki, Noda 278-8510, Chiba 278-8510, Japan
[32]Department of Electronic Information Systems, Shibaura Institute of Technology, 307 Fukasaku, Minuma-ku, Saitama, Saitama 337-8570, Japan
[33]Department of Earth and Space Science, Osaka University, 1-1 Machikaneyama, Toyonaka 560-0043, Osaka, Japan
[34]Department of Physics, University of Wisconsin, 2320 Chamberlin Hall, 1150 University Ave, Madison, WI 53706, USA
[35]University of Waterloo, 200 University Avenue West, Waterloo, Ontario N2L 3G1, Canada
[36]Institut de Recherche en Astrophysique et Planétologie, 9, avenue du Colonel Roche, BP 44346, 31028 Toulouse Cedex 4, France
[37]Department of Physics, Nagoya University, Furo-cho, Chikusa-ku. Nagoya, Aichi 464-8602, Japan
[38]Science Research Education Unit, University of Teacher Education Fukuoka, 1-1 Akamabunkyo-machi, Munakata, Fukuoka 811-4192, Japan
[39]Hiroshima Astrophysical Science Center, Hiroshima University, 1-3-1 Kagamiyama, Higashi-Hiroshima, Hiroshima 739-8526, Japan
[40]Department of Data Science, Tohoku Gakuin University, 3-1 Shimizukoji, Wakabayashi-ku, Sendai, Miyagi 984-8588, Japan
[41]European Space Agency (ESA), European Space Astronomy Centre (ESAC), Camino bajo del Castillo, s/n, Urbanización Villafranca del Castillo, Villanueva de la Cañada, E-28692 Madrid, Spain
[42]Tsukuba Space Center (TKSC), Japan Aerospace Exploration Agency (JAXA), 2-1-1 Sengen, Tsukuba-shi, Ibaraki 305-8505, Japan
[43]Department of Science, Faculty of Science and Engineering, Kindai University, 3-4-1 Kowakae, Higashiosaka, Osaka 577-8502, Japan
[44]Department of Teacher Training and School Education, Nara University of Education, Takabatake-Cho, Nara, Nara 630-8528, Japan
[45]Astronomical Institute, Tohoku University, 6-3 Aramaki, Aoba-ku, Sendai, Miyagi 980-8578, Japan
[46]Department of Physics, Faculty of Science, Nara Women's University, Kitauoya-nishimachi, Nara, Nara 630-8506, Japan
[47]Department of Astrophysics and Atmospheric Sciences, Kyoto Sangyo University, Kamigamo-motoyama, Kita-ku, Kyoto 603-8555, Japan
[48]School of Science and Technology, Meiji University, 1-1-1 Higashi-Mita, Tama-ku, Kawasaki, Kanagawa 214-8571, Japan
[49]Yale Center for Astronomy and Astrophysics, Yale University, PO Box 208120, New Haven, CT 06520-8120, USA
[50]Program of Physics, Department of Science, University of Toyama, 3190 Gofuku, Toyama-shi, Toyama 930-8555, Japan.
[51]Center for Space Science and Technology, University of Maryland, Baltimore County, 1000 Hilltop Circle, Baltimore, MD 21250, USA
[52]Faculty of Science and Engineering, Konan University, 8-9-1 Okamoto, Kobe, Hyogo 658-8501, Japan
[53]Graduate School of Science and Engineering, Kagoshima University, 1-21-40 Korimoto, Kagoshima, Kagoshima 890-8580, Japan
[54]Department of Physics, Chuo University, 1-13-27 Kasuga, Bunkyo-ku, Tokyo 112-8551, Japan
[55]Science Education, Faculty of Education, Shizuoka University, 836 Ohya, Suruga-ku, Shizuoka, Shizuoka 422-8529, Japan
[56]Faculty of Health Science, Nihon Fukushi University, 26-2 Higashihaemi-cho, Handa, Aichi 422-8529, Japan
[57]Anton Pannekoek Institute, the University of Amsterdam, Postbus 942491090 GE Amsterdam, The Netherlands
*Email: tashiro@mail.saitama-u.ac.jp

Abstract

The X-Ray Imaging and Spectroscopy Mission (XRISM) is a joint mission between the Japan Aerospace Exploration Agency (JAXA) and the National Aeronautics and Space Administration (NASA) in collaboration with the European Space Agency (ESA). In addition to the three space agencies, universities and research institutes from Japan, North America, and Europe have joined to contribute to developing satellite and onboard instruments, data-processing software, and the scientific observation program. XRISM is the successor to the ASTRO-H (Hitomi)

mission, which ended prematurely in 2016. Its primary science goal is to examine astrophysical problems with precise, high-resolution X-ray spectroscopy. XRISM promises to discover new horizons in X-ray astronomy. It carries a 6 × 6 pixelized X-ray microcalorimeter on the focal plane of an X-ray mirror assembly (Resolve) and a co-aligned X-ray CCD camera (Xtend) that covers the same energy band over a large field of view. XRISM utilizes the Hitomi heritage, but all designs were reviewed. The attitude and orbit control system was improved in hardware and software. The spacecraft was launched from the JAXA Tanegashima Space Center on 2023 September 6 (UTC). During the in-orbit commissioning phase, the onboard components were activated. Although the gate valve protecting the Resolve sensor with a thin beryllium X-ray entrance window was not yet opened, scientific observation started in 2024 February with the planned performance verification observation program. The nominal observation program commenced with the following guest observation program beginning in 2024 September.

Keywords: instrumentation — space vehicles — space vehicles: instruments — X-rays: general

1 Introduction

The X-Ray Imaging and Spectroscopy Mission (XRISM) (figure 1), the seventh in a series of Japanese X-ray astronomy satellites, was launched by the Japan Aerospace Exploration Agency (JAXA) with the H-IIA launching vehicle from Tanegashima Space Center (TNSC) at 23:47 UTC on 2023 September 6. The launching vehicle H-IIA flight 47 carried two spacecrafts; one was XRISM, and the other was the Smart Lander for Investigating Moon (SLIM). XRISM separated from the vehicle 849 s after launch and entered a near-circular orbit at 575 km altitude with an inclination angle of 31°. Then, XRISM deployed its solar panel arrays and opened the helium vent valve of the observation instrument's onboard coolant to start its critical operations, followed by its commissioning operations. XRISM is a joint mission of JAXA–NASA (US National Aeronautics and Space Administration), conducted in collaboration with the European Space Agency (ESA) and many other institutes in Japan, the United States, Canada, and Europe.

XRISM was proposed as a recovery mission for ASTRO-H (Hitomi). JAXA launched Hitomi on 2016 February 17 and started observation soon after its initial commissioning. However, the attitude control system triggered a series of abnormalities and mishaps that ended the operation. These errors led to a fatal event: the loss of solar panel arrays on Hitomi on 2016 March 26 (Fregel et al. 2017). Despite the short mission life, initial results from Hitomi showed the potential of precise X-ray spectroscopy with imaging for transformative science. For example, measuring energy shifts or line broadening enables precise velocity and dynamic pressure determination in cosmic plasmas. The X-ray microcalorimeter can constrain the Doppler broadening in the iron-K emission line to an accuracy of $\sim$50 km s^{-1}.

Hitomi revealed the velocity of plasmas in clusters of galaxies and various X-ray objects (Hitomi Collaboration 2016, 2018a, 2018e, 2018g, 2018h, 2018i). The high-energy resolution with high throughput leads to unprecedented high sensitivity to the spectral features. The comparison of emission line measurements of the elements, including rare metals, with theoretical calculation, reveals the state of chemical evolution in the source (Aharonian et al. 2017; Hitomi Collaboration 2017, 2018f; Simionescu et al. 2019). A mechanism for X-ray emission, reflecting the physical condition in the source, can also be examined by performing diagnostics in the fine structure of lines (Hitomi Collaboration 2018c, 2018d). Furthermore, the state-of-the-art microcalorimeter is ideal for observing charge exchange, resonance, and Compton scattering in cosmic plasmas (Hitomi Collaboration 2018b). XRISM was developed to provide a multifaceted tool for revealing material circulation and energy transfer in cosmic plasmas and elucidating cosmic structures and evolution.

The four science objectives for XRISM to explore are as follows.

(1) Structure formation of the Universe and evolution of clusters of galaxies:
Galaxies and clusters of galaxies are formed in dark matter halos and evolve into large-scale systems through collisions and mergers. An enormous amount of gravitational energy is released into thermal energy through the kinetic motion of the hot plasma in the systems. XRISM measures plasma velocities to reveal the processes and hidden energy flow channels involved in structure formation.
(2) Circulation history of baryonic matter in the Universe:
Supernova remnants inject thermal and kinetic energy, heavy elements, and high-energy cosmic rays into interstellar and intergalactic space. Thus, these objects are essential in constructing variety in the Universe. The explosions dissipate energy and elements through the gradually thermalized optically thin plasma. Therefore, the plasma diagnosis with high-resolution X-ray spectroscopy is ideal for revealing the dissipation and circulation of baryonic matter in the Universe.
(3) Transport and circulation of energy in the Universe:
The co-evolution of galaxies and their central supermassive black holes is one of the most central modern astronomy themes. Although "co-evolution" is widely accepted, the mass feeding mechanisms on to the supermassive black hole from the host galaxy are still a missing piece of the puzzle. XRISM, with the capability to measure the iron-K emission line energy to an accuracy of $\leq$200 km s^{-1}, resolves velocity fields in the accreting matter, leading to an understanding of the mass feeding structure surrounding the supermassive black hole. Furthermore, outflows, including jets and disk winds, from black holes or other compact objects are essential for understanding energy transportation and circulation in the Universe. XRISM measures the hot plasma flows in the spectral absorption features.
(4) New science with unprecedented high-resolution X-ray spectroscopy:
High-resolution spectroscopy extracts information on the physical state of plasmas that we have not obtained. For example, the plasma diagnosis of the fine spectral features enabled by XRISM provides an understanding of the history of plasma ionization. High-resolution spectroscopy can probe gravitational redshifts in relativistic objects. These new observable properties will expand new areas of astrophysics.

XRISM is designed to fulfill these scientific objectives with high-resolution X-ray spectroscopy with imaging by

Fig. 1. Outlook of XRISM and onboard mission instruments. Two X-ray mirror assemblies and three star tracker units are equipped on the top plate on the upper left. The solar panel arrays are the dark wing-shaped structures in the center. Credit: JAXA.

Table 1. Key parameters of the spacecraft.

Launch site	Tanegashima Space Center, Japan
Launch vehicle	JAXA H-IIA rocket
Orbit type	Approximate circular orbit
Altitude	575 ± 15 km
Orbit inclination	31°
Dimension	7.9 m × 9.2 m × 3.1 m
Mass	2.3 t
Design life	≥3 yr

observing the fine structure in the X-ray spectra and the spatial distribution of cosmic plasmas (Tashiro et al. 2018).

2 Spacecraft

2.1 The orbit and operations

The satellite operation is conducted at the Sagamihara Satellite Operation Center of ISAS/JAXA, using the ground station at the Uchinoura Space Center (USC) in Japan. The key parameters of the spacecraft are summarized in table 1. The spacecraft circulates the Earth for 96 min on a near-Earth orbit and contacts the ground station, USC, on 5 out of the 15 daily orbits. XRISM employs the JAXA Global Network (GN) stations, the NASA Near Space Network (NSN) stations, and the nominal operation station USC. The additional GN and NSN stations cover most of the remaining 10 orbits to monitor the spacecraft's essential status.

The basic observation pattern is to point to an object during the planned exposure time and then slew to the next target. Each typical XRISM observation is expected to take one to a few days, and the command plan for each observation is uploaded during the daily contact with the USC station. The XRISM Mission Operation Team of JAXA oversees the satellite operation by commanding and downlinking data. Collaborating with the Mission Operation Team, the XRISM Science Operations Team (SOT), consisting of dedicated duty scientists, oversees observation planning, science data processing, distribution, archiving, and user support. The XRISM SOT comprises members from three agencies: the XRISM Science Operation Centre (SOC) in JAXA, the XRISM Science Data Center (SDC) in NASA, and members from the European Space Astronomy Centre (ESAC) of ESA. Detailed descriptions of the science operations are given in separate papers (Terada et al. 2021; Holland et al. 2025; Hayashi et al. 2025).

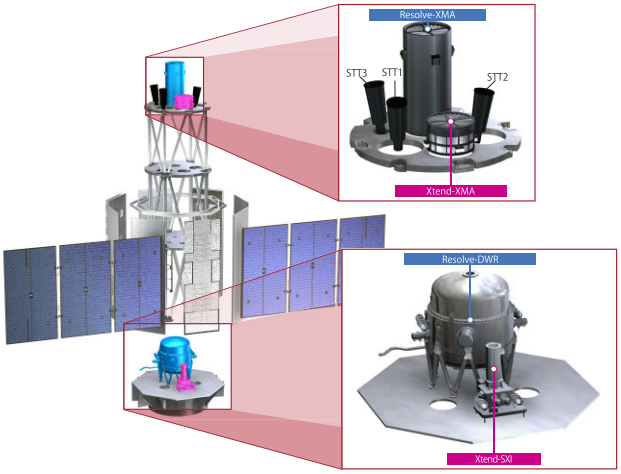

Fig. 2. XRISM onboard mission instruments. Two X-ray mirror assemblies are mounted on the top plate of the spacecraft for the two telescopes, Resolve and Xtend. The focal plane detectors—Resolve sensors in the Resolve dewar (Resolve-DWR) and the CCD in the Xtend-SXI—are installed on the base plate. The three star trackers (STTs) are equipped on the top plate. Credit: JAXA.

2.2 Configuration of the spacecraft

XRISM carries two sets of X-ray telescopes named Resolve and Xtend. As shown in figure 2, XRISM is equipped with two sets of co-aligned X-ray mirror assemblies (XMAs) and two sets of star sensors (star trackers: STT) to the right of the XMAs. Behind the central XMA, we see part of the sunshade from the third STT. The side panels, equipped with electronics inside, shape an octagonal pillar. The two sets of science instrument detectors are on the spacecraft's base plate and are surrounded by the side panels. On the side panel opposite the black solar panel arrays is a truss structure between two gray thermal radiators. The dewar (Resolve-DWR) containing the X-ray microcalorimeter is installed at the back of the structure, facing the anti-solar direction, and the radiators connected by heat pipes provide effective radiative cooling of the dewar surface. The CCD camera of Xtend (Xtend-SXI) is placed inside the spacecraft and is connected to its radiator via two heat pipes.

Figure 3 shows a function block diagram of XRISM. The bus system consists of the power supply, communication and data handling, and attitude orbit control subsystem. The above right portion of the figure shows components for the science instruments. As the primary design policy, we require the spacecraft bus system to be designed to be one-fail-operative. According to the policy, almost all the bus electronics components configure redundant systems, as indicated by the overlapping rectangles. The only exceptions are the electronics for the global positioning system receiver (GPSR) and the X-band transponder. They are single systems but functionally redundant with the on-ground time assignment/orbit determination systems or S-band communication. The X band has about four times the bandwidth of the S band and is used to download accumulated observation data, although the ground stations that we use to receive it are limited to those in Japan. When the X band is not available, we use the S band to

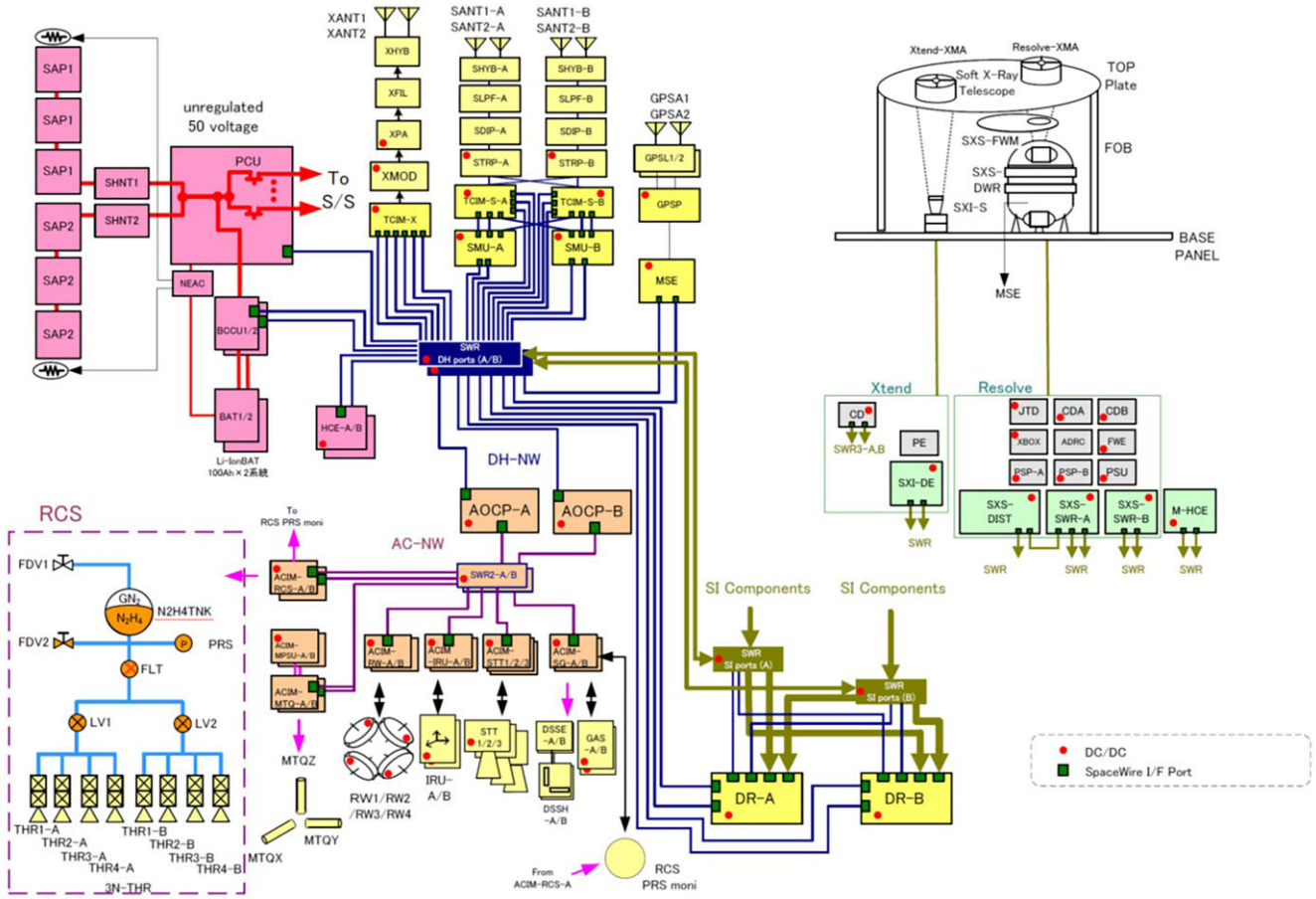

Fig. 3. Function block diagram of XRISM. The upper-left block shows the solar panels and power supply units and the communication and data handling components. The attitude and orbital control components are shown at the bottom. The mission instruments are shown in the top right. SpaceWire is employed for onboard communication. Credit: JAXA

accumulate observation data also using overseas station networks.

2.3 Attitude control system

XRISM is a three-axis stabilization satellite pointing at a celestial object with telescopes and fixed solar panels facing the Sun. Therefore, the attitude and orbit control system (AOCS) is crucial for both the mission and spacecraft survival. The AOCS is composed of attitude sensors, data processors, and actuators.

The attitude sensors consist of four independent components: digital Sun sensors (DSSs), geomagnetic attitude sensors, inertial reference units, and STTs. The solar panels are fixed to the spacecraft and restrict attitude operation to keep the normal against the Sun inclination angle within 30° on orbit. The DSS measures the Sun angle against the solar panels to maintain the power generation. The linear measurement range is a ±64 squared degree region. The area is much broader than that of Hitomi to cover the Sun inclination angles with enough margin. The pointing accuracy is assured by the attitude determination using the star sensors (STTs) installed on the top plate with the XMAs. Figure 4 shows the STT fields of view and avoidance angles for interfering light from Earth's albedo. The view centers are offset from the normal of the top panel by 10°, and the position angles of the STTs are separated by 120°. With this configuration, the STTs cover a broad field

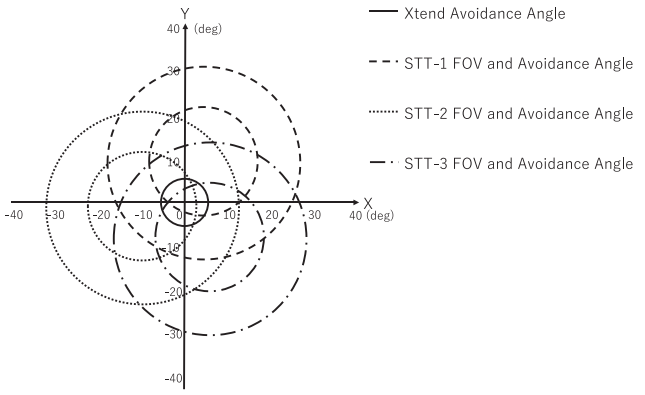

Fig. 4. Fields of view (12.5 in radius) and avoidance angles (22° in radius) for interfering light of the three STTs and the avoidance angle of Xtend (the smallest circle at the center). The three STTs cover overlapping broad fields of view to realize accurate and robustness in attitude control.

of view, avoiding the Earth occultation to realize an extended time coverage for the attitude determination with the STTs. Also, simultaneous measurement with two or three STTs increases the attitude determination accuracy to ≤20″ through the on-ground attitude determination process.

The actuators are reaction wheels and thrusters (reaction control systems). The former is the primary actuator

stabilizing or pointing the telescopes to the target. In contrast, the latter points to the satellite at the first Sun acquisition after the satellite separation and emergency safehold operation. The magnetic torquers dissipate the angular momentum accumulated in the reaction wheels.

In addition to the regular attitude control operation and debris avoidance maneuver, one of the most crucial functions of the data processor on the attitude control system is the fault detection isolation and reconfiguration (FDIR) system. Each component employs reliable parts (level 4) and error detection and correction systems in the data transfer lines (level 3). The RMAP/SpaceWire network protocols ensure communication between components (level 2). The attitude and orbit control flight software (ACFS), installed in the data processor, monitors hardware and inter-component consistency by comparing the sensor output values. Once a hardware error or inter-component inconsistency is detected, the ACFS switches the whole system to the redundant side (level 1). The lower-level hardware/system quickly detects a definite abnormality in each component and automatically switches to the redundant system. In contrast, the ACFS detects inter-component inconsistency at a higher level to isolate and reconfigure the AOCS. By separating each fault detection and reconfiguration function level, the system avoids congestion and a chain of abnormality faults.

The initial stage of FDIR is a fault-tolerant or fail-operational mode. In these levels, the spacecraft continues pointing operations by resetting or switching to the redundant system. However, if the fault is not corrected in the initial stage, the attitude control mode is changed to safehold mode. In this mode, the pointing operation is free-spinning around the $+Y$ axis (the normal of the solar panel), and the angular moment is controlled to direct the $+Y$ axis to the Sun. Momentum wheels control the safehold at first. If this fails, the attitude control actuator is switched to the thrusters. However, the AOCS cuts the thruster at the last stage when it detects a high angular velocity to prevent the spacecraft from breaking up. After the cutoff, there is no active actuator controlled by the onboard AOCS. The spacecraft would be saved by commands from the ground-support stations.

3 Mission instruments

XRISM carries two science instruments: the Resolve soft X-ray spectrometer and the Xtend soft X-ray imager, as mentioned in subsection 2.2. Two identical XMAs mounted on the spacecraft top plate are conically approximated Wolter I optics consisting of 203 nested shells, following the basic design for the Hitomi soft X-ray telescopes (SXTs) (Soong et al. 2014). The ground-calibration results are shown by Boissay-Malaquin et al. (2022), Tamura et al. (2022), and Hayashi et al. (2022).

Resolve has an X-ray microcalorimeter array that delivers ∼5 eV energy resolution at an operational temperature of 0.05 K maintained by six stages of cooling (Kilbourne et al. 2018; Ezoe et al. 2020; Ishisaki et al. 2022). The basic design of the X-ray microcalorimeter and the cooling system follows that of the SXS onboard Hitomi, though newly developed mechanisms are adopted in the gate valve (GV) and vibration interference isolators (VIS) (Yasuda et al. 2025). We installed an eddy current dumper in the GV opening mechanism. The GV protects the sensor in the vacuum dewar from the atmosphere and shall be opened in orbit. The eddy current dumper controls the opening speed and reduces the shock to the thermal shield films before the sensor. On the other hand, the VIS is installed between the mechanical cooler compressor and the dewar and restricts the vibration noise from propagating to the sensor. The isolation mechanism is redesigned for the spacecraft mechanical environment of XRISM at the launch and spacecraft separation. A detailed description is given in Midooka et al. (2020). The status of development and the on-ground calibration are reported in Porter et al. (2020) and Eckart et al. (2024).

The Xtend X-ray CCD camera delivers a broad field of view with a moderate energy resolution (Hayashida et al. 2018; Mori et al. 2022; Noda et al. 2025). The basic design of the CCD camera is identical to that of the Hitomi SXI, and some improvements are adopted on the CCD chip and the scheme for preventing light leakage. The development and on-ground calibration status are reported by Nakajima et al. (2020), Uchida et al. (2020), Yoneyama et al. (2020), and Kanemaru et al. (2020). The key parameters, in-orbit operations and verified performance are summarized in subsection 4.3 and Mori et al. (2024), Suzuki et al. (2025b), and Uchida et al. (2025).

4 In-orbit operation and observations

4.1 Launch phase

XRISM was initially scheduled to launch in 2023 May. However, launch operations were suspended by JAXA to evaluate the countermeasure of the H3 launch vehicle accident.[1] Launch operation resumed at Tanegashima Space Center in 2023 July. After a series of function checks, we conducted a launch-day dry run on August 18. On August 21, the superfluid liquid helium in the Resolve dewar helium tank was filled to cool the dewar insert in preparation for launch. The final launch preparation review was held on August 24, and the spacecraft and launch vehicle were ready for launch. However, the launch was postponed due to unfavorable weather conditions and was finally rescheduled to September 6.

XRISM was launched successfully and separated from the launch vehicle in the sky over the Pacific Ocean. The NASA USHI station in Hawaii confirmed the separation signal from the launch vehicle at the 0th orbit. Satellite operations are conducted at the Sagamihara Space Operation Center of ISAS/JAXA using the JAXA and NASA ground-station networks. The spacecraft orbits the Earth for 96 min in a low-Earth orbit, and a ground station contacts the spacecraft in about 5 out of 15 orbits per day. We extend the coverage using JAXA GN and NASA NSN stations.

4.2 Critical operations

After separation from the launch vehicle, the completion of the Sun acquisition was confirmed. The launch lock of the vibration isolation system of the four mechanical coolers (two shield coolers and two precoolers) of Resolve was unlocked by a "real-time" command operation in the first contact by Santiago station. In the second revolution orbit, we switched the Sun tracking mode from the reaction control system to the reaction wheels. After stabilizing the attitude to point the solar arrays at the Sun, we started the Resolve mechanical coolers. At the 30th revolution, we confirmed that the Resolve

[1] JAXA press release, 2023 March 7 ⟨https://global.jaxa.jp/press/2023/03/20230307-2_e.html⟩.

Table 2. Key parameters and performance of the payload instruments.

Parameter	Resolve	Xtend
X-ray mirrors	Conically approximated Wolter I optics (203 nested shells)	
Focal length	5.6 m	
Detector technology	X-ray microcalorimeter	X-ray CCD
Field of view	3′.1 × 3′.1	38′.5 × 38′.5
Sensitive band	1.7*–12 keV	0.4–13 keV
Effective area	180 cm^2 @ 6 keV*	∼420 cm^2 @ 1 keV, ∼310 cm^2 @ 6 keV
On-axis XMA PSF at 6.4 keV	1′.3 (HPD), 7″.9 (FWHM)	1′.4 (HPD), 7″.2 (FWHM)
Pixel size	30″ × 30″ (818 μm)	1″.77 (48 μm, pixel size)
Time resolution	5 μs (high- and mid-res), 80 μs (lo-res)	4 s (full window), 0.5 s (1/8 window)
Absolute time tagging accuracy	<1 ms	—
Energy resolution	4.5 eV FWHM (high-res)† @ 6 keV 4.8 eV FWHM (mid-res primary)†	∼180 eV FWHM @ 6 keV
Absolute energy scale	<1 eV (1.7–12 keV) <0.3 eV (5.4–9.0 keV high-res)	—
Count-rate limit	200 counts s^{-1} $array^{-1}$	3 mCrab (full window)
Non X-ray background	7×10^{-4} counts s^{-1} keV^{-1} $array^{-1}$ (1–12 keV)	$\leq 1 \times 10^{-6}$ counts s^{-1} keV^{-1} $arcmin^{-2}$ cm^{-2} (5–12 keV)

*In the closed gate valve configuration.
†Focal plane average.

dewar shield cooler temperature stabilized the shield temperature at 4.5 K.

4.3 Commissioning

The following functions and performance were evaluated and verified to ensure normal operation, including items verified during the critical operation period. These are power generation and control, telemetry command ranging via the S band, receiving observation data via the X band, data recording and playback, orientation accuracy and attitude pointing, attitude control, temperature control, GPS function, and time distribution function. The verification of the optical axis alignment with the attitude control system is described by Kanemaru et al. (2025).

Following the bus components, Resolve began functional and performance verification on October 7. The adiabatic demagnetization refrigerator (ADR) was powered up and cooled from 5 K to 50 mK (Chiao et al. 2024). The mechanical coolers' operation frequency was tuned to minimize microvibration interference with the Resolve sensor (Sneiderman et al. 2024). On November 7, we conducted the first attempt to open the GV. However, the GV did not deploy after this operation or after two successive attempts in November and December. Due to the 250 μm thick Be window mounted on the GV, the Resolve's low-energy band is limited to energies above 1.7 keV. See the XRISM proposers' observatory guide for a detailed description of the effect of closed valves on the observation band.[2] As we see in the next section, the XRISM project started the science observations with the GV closed because we confirmed the science productivity. The XRISM project continues to investigate the countermeasures taken after the unsuccessful operation and the operational plan for retrying the valve-opening operation in the future before the cryogen-free mode of Resolve. Resolve is equipped with multiple types of calibration sources on the filter wheel (FW) for tracking the gain drift of the detector pixels in the orbit (Shipman et al. 2024). The baseline plan of the gain tracking was to use active calibration sources called modulated X-ray sources (MXS). However, because of the GV aperture structure, the MXS cannot irradiate all the pixels at once. Therefore, currently the gain tracking is performed by intermittently irradiating the ^{55}Fe radioactive sources on the FW, based on the backup plan prepared before the launch and implemented in the commissioning (Sawada et al. 2024), which has been working successfully (Eckart et al. 2024). Along with the gain tracking and calibration method, the event screening method and criteria were established and verified (Mochizuki et al. 2025).

We also conducted the commissioning of each component of the Xtend system. We started the mechanical coolers from October 17–22 and adjusted the parameters to confirm that they operated normally. From November 2–12, we conducted observations with the 1/8 window mode and 1/8 window+burst mode to verify the window position (Suzuki et al. 2025b). Xtend was aligned in window mode based on the result of the Resolve central-axis calibration.

In parallel with the onboard instrument commissioning, on-ground science operations were established as planned. The science observation planning procedures and data-processing pipelines were tested, improved, and verified in collaboration between the SOC, SDC, and ESAC, supported by JAXA, NASA, and ESA (Holland et al. 2025; Hayashi et al. 2025).

The XRISM In-Flight Calibration Planning Team, in collaboration with the instrument development teams, planned the mission instrument calibration. The on-orbit celestial object calibration was carefully selected for each calibration item and revised to meet the closed gate condition. The policy and plan are described by E. D. Miller et al. (in preparation). In addition to the high-resolution spectroscopy and the wide-field imaging mentioned above, timing accuracy is an essential capability of XRISM, especially for Resolve with the time resolution of 5 μs. The time assignment accuracy is also verified to meet the requirements (Terada et al. 2025; Shidatsu et al. 2025; Sawada et al. 2025). The key parameters and performance of the mission instruments are summarized in table 2.

4.4 First light observations

The first light for Xtend was performed from October 14–24 as part of the initial functional verification. The cluster Abell

[2] ⟨https://heasarc.gsfc.nasa.gov/docs/xrism/proposals/POG/xrism_pog.pdf⟩.

2319 was observed, and X-ray images were successfully obtained.[3] The X-ray image shows a broad field of view covering the entire galaxy cluster and serendipitous sources outside the cluster region. The image resolution is good enough to resolve the structure of the merging clusters. The detailed performance of the XMAs for Resolve and Xtend is reported by Hayashi et al. (2024) and Tamura et al. (2024).

As part of the initial functional verification and calibration operation, first light observations were conducted from December 4–11 to observe the supernova remnant N 132D in the Large Magellanic Cloud, obtaining a detailed X-ray spectrum (XRISM Collaboration 2024c). Although the closed gate valve limits the soft X-ray band, the spectrum shows emission lines from silicon to iron with high signal-to-noise values. The measured spectral resolution of ∼4.5 eV (FWHM at 6 keV) makes it possible to resolve many lines from ions of various elements. The first paper was published by the XRISM Collaboration (2024c) and was followed by a series of papers on observations of NGC 4151, Cyg X-3, or other sources (e.g., XRISM Collaboration 2024a, 2024b).

4.5 Observation phases

After commissioning, we began the planned performance verification observations on 2024 February 7. Although the observing targets had been selected before launch, the list was modified to account for the closed GV's band limitation. The revised target list is available to researchers on the XRISM website.[4] During the performance verification phase, the observed data rights belong to the XRISM science team, with a limited number of XRISM guest scientists invited by the three space agencies.

XRISM serves as an observatory for the global community through the dedicated guest observation program. JAXA, NASA, and ESA independently issued a call for proposals in 2023 November. The XRISM GO cycle-1 approved target list was opened in 2024 July, and the guest observations started in 2024 September. The first five months were used for commissioning, checking out, and essential calibration of the bus and mission components. Guest observations from the global astronomical community will continue until at least 2026 September. The nominal operational phase of XRISM is defined as the first three years after launch. The later phase operation will be defined after the review of the nominal operation.

Several scientific results have already been published (e.g., Mochizuki et al. 2024; XRISM Collaboration 2025a, 2025b; Suzuki et al. 2025a; Tsujimoto et al. 2025), and more are in preparation for publication. Many more results are expected to follow. In addition to the programmed pointing observations, the Xtend's broad field of view allows us to add science by searching transient X-ray sources in the field. The Xtend transient search activity and the early results are shown in Tsuboi et al. (2025).

Acknowledgments

We owe XRISM's success to the dedication and high capability of the many people who have worked on this project for many years, since the time of ASTRO-E, ASTRO-E2 (Suzaku), and ASTRO-H (Hitomi). The XRISM team is deeply grateful to the XRISM External Science Advisory Panel—Prof. Andrew Fabian, Dr. Nancy Brickhouse, Dr. Jan-Willem den Herder, Dr. Gerard Kriss, and Prof. Tadayuki Takahashi—for the varied and constructive advice that they have given us based on their experience.

XRISM is being developed through an international collaboration between the Japan Aerospace Exploration Agency (JAXA), the National Aeronautics and Space Administration (NASA), and the European Space Agency (ESA). In addition to the three space agencies, universities and research institutes from Japan, the United States, and Europe have joined to contribute to developing satellites, science instruments, and data-processing software and further formulate scientific observation plans. Our science activity was partly supported by the JSPS Core-to-Core Program (grant number: JPJSCCA20220002).

[3] JAXA press release, 2024 January 5 ⟨https://global.jaxa.jp/press/2024/01/20240105-1_e.html⟩.

[4] ⟨https://xrism.isas.jaxa.jp/research/⟩.

References

Aharonian, F. A., et al. 2017, ApJ, 837, L15
Boissay-Malaquin, R., et al. 2022, Proc. SPIE, 12181, 121811U
Chiao, M. P., Bialas, T. G., Ray, K. A., DiPirro, M. J., Kilbourne, C. A., Porter, F. S., Shirron, P. J., & Sneiderman, G. A. 2024, Proc. SPIE, 13093, 1309361
Eckart, M. E., et al. 2024, Proc. SPIE, 13093, 130931P
Ezoe, Y., et al. 2020, Cryogenics, 108, 103016
Fregel, S., Bennett, J., Lachut, M., Möckel, M., & Smith, C. 2017, Earth Planets Space, 69, 51
Hayashi, T., et al. 2025, J. Astron. Telesc. Instrum. Syst., submitted
Hayashi, T., et al. 2022, Proc. SPIE, 12181, 121815Y
Hayashi, T., et al. 2024, Proc. SPIE, 13093, 130931L
Hayashida, K., et al. 2018, Proc. SPIE, 10699, 1069923
Hitomi Collaboration 2016, Nature, 535, 117
Hitomi Collaboration 2017, Nature, 551, 478
Hitomi Collaboration 2018a, PASJ, 70, 9
Hitomi Collaboration 2018b, PASJ, 70, 10
Hitomi Collaboration 2018c, PASJ, 70, 11
Hitomi Collaboration 2018d, PASJ, 70, 12
Hitomi Collaboration 2018e, PASJ, 70, 13
Hitomi Collaboration 2018f, PASJ, 70, 14
Hitomi Collaboration 2018g, PASJ, 70, 16
Hitomi Collaboration 2018h, PASJ, 70, 17
Hitomi Collaboration 2018i, PASJ, 70, 38
Holland, M., et al. 2025, J. Astron. Telesc. Instrum. Syst., submitted
Ishisaki, Y., et al. 2022, Proc. SPIE, 12181, 121811S
Kanemaru, Y., et al. 2020, Nucl. Instrum. Methods Phys. Res. A, 984, 164646
Kanemaru, Y., et al. 2025, J. Astron. Telesc. Instrum. Syst., submitted
Kilbourne, C. A., et al. 2018, J. Astron. Telesc. Instrum. Syst., 4, 011214
Midooka, T., et al. 2020, Proc. SPIE, 11444, 114445C
Mochizuki, Y., et al. 2024, ApJ, 977, L21
Mochizuki, Y., et al. 2025, J. Astron. Telesc. Instrum. Syst., in press
Mori, K., et al. 2022, Proc. SPIE, 12181, 121811T
Mori, K., et al. 2024, Proc. SPIE, 13093, 1309331I
Nakajima, H., et al. 2020, Proc. SPIE, 11444, 11444177
Noda, H., et al. 2025, PASJ, in press
Porter, F. S., et al. 2020, Proc. SPIE, 11444, 1144424
Sawada, M., et al. 2025, J. Astron. Telesc. Instrum. Syst., submitted
Sawada, M., et al. 2024, Proc. SPIE, 13093, 1309364
Shidatsu, M., et al. 2025, J. Astron. Telesc. Instrum. Syst., submitted
Shipman, R. F., et al. 2024, Proc. SPIE, 13093, 130935W
Simionescu, A., et al. 2019, MNRAS, 483, 1701
Sneiderman, G. A., Chiao, M. P., Kilbourne, C. A., Porter, F. S., & Tsujimoto, M. 2024, Proc. SPIE, 13093, 1309369
Soong, Y., et al. 2014, Proc. SPIE, 9144, 914428
Suzuki, H., et al. 2025a, ApJ, 978, L20
Suzuki, H., et al. 2025b, J. Astron. Telesc. Instrum. Syst., submitted

Tamura, K., et al. 2022, Proc. SPIE, 12181, 121811V
Tamura, K., et al. 2024, Proc. SPIE, 13093, 130931M
Tashiro, M., et al. 2018, Proc. SPIE, 10699, 1069922
Terada, Y., et al. 2021, J. Astron. Telesc. Instrum. Syst., 7, 037001
Terada, Y., et al. 2025, J. Astron. Telesc. Instrum. Syst., in press
Tsuboi, Y., et al. 2025, J. Astron. Telesc. Instrum. Syst., submitted
Tsujimoto, M., et al. 2025, PASJ, in press
Uchida, H., et al. 2020, Nucl. Instrum. Methods Phys. Res. A, 978, 164374
Uchida, H., et al. 2025, J. Astron. Telesc. Instrum. Syst., submitted
XRISM Collaboration 2024a, ApJ, 973, L25
XRISM Collaboration 2024b, ApJ, 977, L34
XRISM Collaboration 2024c, PASJ, 76, 1186
XRISM Collaboration 2025a, Nature, 638, 365
XRISM Collaboration 2025b, PASJ, 77, L1
Yasuda, S., et al. 2025, J. Astron. Telesc. Instrum. Syst., in press
Yoneyama, T., et al. 2020, Proc. SPIE, 11444, 1144425

Received: 2025 February 1; Accepted: 2025 March 14